IAI Accepts, published online ahead of print on 2 September 2014
Infect. Immun. doi:10.1128/IAI.02284-14

Rat Indwelling Urinary Catheter Model of *Candida albicans* Biofilm Infection

Jeniel E. Nett[1,2], Erin Brooks[3], Jonathan Cabezas-Olcoz[1], Hiram Sanchez[1], Robert Zarnowski [1], Karen Marchillo[1,2], David R. Andes[1,2*]

University of Wisconsin, Department of Medicine[1], Department of Medical Microbiology and Immunology[2], Department of Pathology and Laboratory Medicine[3]

Running title: *Candida* urinary catheter biofilm model

* 5211 UW Medical Foundation Centennial Building
1685 Highland Ave
Madison, WI 53705
phone (608) 263-1545
fax (608) 263-4464
dra@medicine.wisc.edu

ABSTRACT

Indwelling urinary catheters are commonly used in the management of hospitalized patients. *Candida* can adhere to the device surface and propagate as a biofilm. These communities differ from free-floating *Candida*, exhibiting high tolerance to antifungal therapy. The significance of catheter-associated candiduria is often unclear and treatment may be problematic considering the biofilm drug resistant phenotype. Here we describe a rodent model for study of urinary catheter-associated *Candida albicans* biofilm infection that mimics this common process in patients. In the setting of a functioning, indwelling urinary catheter in a rat, *Candida* proliferated as a biofilm on the device surface. Characteristic biofilm architecture was observed, including adherent, filamentous cells embedded in an extracelluar matrix. Similar to patients, animals with this infection developed candiduria and pyuria. Infection progressed to cystitis and a biofilm-like covering was observed over the bladder surface. Furthermore, large numbers of *C. albicans* were dispersed into the urine from either the catheter or bladder wall biofilm over the infection period. We successfully utilized the model to test the efficacy of antifungals, analyze transcriptional patterns, and examine the phenotype of a genetic mutant. The model should be useful for future investigations involving the pathogenesis, diagnosis, therapy, prevention, and drug resistance of *Candida* biofilms in the urinary tract.

INTRODUCTION

Hospitalized patients frequently develop urinary tract infections. Catheter-associated urinary tract infection (CAUTI) is the most prevalent nosocomial infection, with over 1 million patients diagnosed yearly in the United States (1-3). *Candida* spp. account for the third most common cause of infection (2, 4, 5). Many factors have been linked to candiduria, including diabetes, urological procedures, female sex, and urological devices (6). Urinary catheters, devices necessary for monitoring the output of urine and maintaining urine outflow, are used in up to 20% of all hospitalized patients (7). Catheters provide a substrate for adherence of microorganisms and proliferation of biofilms. When growing as a biofilm, *Candida* is difficult to eradicate due to inherent drug-resistance and immune tolerance (8-12).

The identification of *Candida* in the urine can indicate one of several clinical processes (13). The question of how to differentiate among these scenarios and optimally manage candiduria remains controversial (6, 14). First, *Candida* may enter the urinary tract from the mucosal surface, adhere to the urinary catheter, and establish a biofilm. Without further invasion, most patients are asymptomatic. However, *Candida* may produce cystitis or ascend further, reaching the kidneys, producing pyelonephritis. These infections are often symptomatic and require antifungal treatment. In another scenario, candiduria may be a sign of disseminated candidiasis with shedding of organisms from hematogenously

seeded kidneys. Alternatively, candiduria may be the result of a contamination of urine, which may occur in the setting of vaginal candidiasis.

Diagnostic tools to differentiate among these clinical states are inadequate and as a result, many patients receive unnecessary antifungal therapy (6, 15, 16). Models for study of CAUTI and candiduria would be of great value for investigating the pathogenesis of these various clinical presentations. The discovery of diagnostic markers to predict which patients may benefit most from treatment would help clinicians decipher urinary culture results and optimally utilize antifungal therapies.

Here, we describe a model for *C. albicans* biofilm infection of a urinary catheter in a rat. This model mimics *Candida* infection of an indwelling urinary catheter in patients. The model represents the clinical scenario with regard to anatomic location, urine flow, and common silicone device material. Over the course of infection, the animals develop progressive candiduria and urinalysis demonstrates inflammation. Ultimately, pathologic findings are consistent with cystitis. On microscopic examination, mature biofilms cover the catheter surface. Our findings suggest this model will be useful for investigations of biofilm pathogenesis and host response to this common clinical infection.

MATERIALS AND METHODS

Organisms and inoculum. *Candida albicans* strains K1, DAY185, and *als1-/- als3-/-* were used for studies (17-19). The strains were stored in 15% (vol/vol) glycerol stock at -80^{o}C and maintained on yeast extract-peptone-dextrose (YPD) medium + uridine (1% yeast extract, 2% peptone, 2% dextrose, and 80 µg/ml uridine) prior to experiments. Prior to catheter inoculation, cells were grown at 30^{o}C in YPD + uridine liquid media with orbital shaking at 200 RPM overnight. To prepare inoculum, cells were enumerated by hemocytometer counting and resuspended in YDP at 10^{8} cells/ml. Final inoculum concentration was confirmed by microbiologic enumeration.

Animals and catheter maintenance. Specific-pathogen-free female Sprague-Dawley rats weight 350 g (Harlan Sprague-Dawley, Indianapolis, Ind.) were used for all studies. Animals were maintained in accordance with the American Association for Accreditation of Laboratory Care criteria and all studies were approved by the institutional animal care committee. On the day of catheter placement, animals received a single dose of cortisone acetate 250 mg/kg subcutaneously. Animals also received and gentamicin 80 mg/kg subcutaneously twice daily and drinking water containing penicillin G sodium (0.9 mg/ml). Dosing regimens were chosen based upon those previously shown to be effective in treatment of rodent systemic bacterial infections (Andes lab, unpublished data). During the period of catheter placement, animals were maintained in metabolic cages. The animals were examined for signs of distress every 6 h throughout the

study. The catheter sites were examined twice daily for signs of inflammation or purulence.

Urinary catheter placement and infection. Rats were anesthetized by intraperitoneal injection (1 mg/kg) of a mixture of xylazine (AnaSed; Lloyd Laboratories, Shenadonoah, Iowa) (20 mg/ml) and ketamine (Ketaset; Aveco Co., Fort Dodge, Iowa) (100 mg/ml) in a ratio of 1:2 (vol/vol). Animals were surgically prepped from midline to tail using surgical scrub (4% parachlorometaxylenol). A silicone catheter (Instech Solomon, 3.5Fr, female luer, round tip, 60 cm, gas sterilized) was inserted in the urethra and advanced to the first marking and secured with surgical glue (VetClose Surgical Glue, Butler Shein Animal Health) (**Figure 1**). Following device placement, a protective covering and button (Polysolfone Button Tether, Instech Solomon) was advanced over the catheter and secured to the subcutaneous tissue by nylon suture (4-0) using 3 interrupted surgical knots. In addition, the animal was placed in a rodent jacket and Elizabethan collar (Braintree Scientific) to prevent animal manipulation of the urinary device. Using a syringe, urine was drained from the bladder though the catheter. Next, 700 µl of culture (the entire catheter volume) was instilled in to the catheter lumen for 2 hours. During this time, the animal was placed on heated blanket and monitored for signs of distress. After 2 hours, the inoculum was removed and the animal was placed in a metabolic cage. The catheter in the protective covering was threaded through the wire floor of the cage. The distal catheter was inserted into a 15 ml plastic conical tube through a

hole in the lid and secured with a bolt and washer. Recovery of the animal after the catheter surgery was assessed according to a standard protocol approved by the Veterans Administration Animal Committee. After 24-72 hours, the animals were euthanized and catheters and/or bladders were collected for analysis, as described below.

Fungal cultures and urinalysis. To determine the viable burden of *C. albicans*, microbiologic counts were performed on urine, urinary catheters, and bladders. Urinary catheters were placed in 2 ml 0.15M NaCl, sonicated for 10 min (FS 14 water bath sonicator and 40 kHz transducer [Fisher Scientific]), and vortexed for 30 s. Dilutions (1:10) were plated in duplicate or triplicate on Sabouraud dextrose agar (SAB). Urine analysis for leukocyte esterase and red blood cells was performed using a commercial urine dipstick (Rapid Response Urinalysis reagent strips, BTNX Inc.) after 24, 48, and 72 hours of infection.

Scanning electron microscopy (SEM). Urinary catheters were processed for SEM as previously described for venous catheters (17). Urinary catheters were harvested at 48 h. Following removal, the distal segment (bladder and urethral portion) was placed in fixative (1% [vol/vol] glutaraldehyde and 4% [vol/vol] formaldehyde in PBS) overnight. The samples were washed with PBS, placed in 1% osmium tetroxide buffered with PBS for 30 min, and rinsed with PBS. The samples were subsequently dehydrated with a series of ethanol washes (30% for 10 min, 50% for 10 min, 70% for 10 min, 95% for 10 min, and 100% for 10 min)

and desiccation was performed by critical-point drying (Tousimis, Rockville, Md.). Specimens were mounted on aluminum stubs and sputter coated with gold. Samples were imaged in a scanning electron microscope (SEM LEO 1530) at 3 kV. The images were processed for display using Adobe Photoshop.

Histopathology. To evaluate the host response to *C. albicans* infection of the urinary catheter, we examined bladder wall histopathology. Animals were sacrificed at 48 hours. The urinary catheters were removed and bladders were dissected, fixed in 10% buffered formalin, and embedded in paraffin (20). Sections were stained with hematoxylin and eosin (H&E) and Gomori's methenamine silver (GMS) for imaging of *Candida*. Images were obtained at 10x and 40x. For SEM, bladders were fixed in phosphate buffered 1.5% glutaraldehyde solution and otherwise processed and imaged for SEM as described above.

Antifungal treatments. The effect of antifungal therapy on viable *C. albicans* biofilms was assessed by systemic treatment of mature biofilm infections (24h incubation) for 2 days. Animals were treated with either fluconazole 25 mg/kg subcutaneously once daily or amphotericin B deoxycholate 1 mg/kg intraperitoneally once daily and compared to untreated controls. At the completion of therapy, animals were sacrificed. The catheters and bladders were removed and the viable *Candida* burden was determined as described above.

183 Microbiologic assays were performed in triplicate and significant differences were
184 measured by ANOVA with pair-wise comparisons using the Holm-Sidak method.
185
186 **RNA collection and quantitative RT-PCR.** Urinary catheters were collected for
187 RT-PCR analysis after 24 hours of growth and placed in RNA later (Qiagen).
188 Biofilm cells were dislodged from the catheter by vortexing, and sonication. RNA
189 was purified using the RNeasy Minikit (Qiagen) and quantified using a NanoDrop
190 spectrophotometer. TaqMan primer and probe sets designed using Primer
191 Express (Applied Biosystems, Foster City, CA) for *ACT1*, *FKS1*, *BGL2*, *XOG1*,
192 and *PHR1* were used as previously described (Supplementary Table 1) (21).
193 These genes were chosen based upon differential expression in the vascular
194 catheter and denture biofilm models (21, 22). The QuantiTect probe RT-PCR kit
195 (Qiagen) was used in a CFX96 real-time PCR detection system (Bio-Rad) with
196 the following program: 50°C for 30 min, initial denaturation at 95°C for 15 min,
197 and then 40 cycles of 94°C for 15 s and 60°C for 1 min. Reactions were
198 performed in triplicate. The expression of each gene relative to that of *ACT1* is
199 presented. The quantitative data analysis was completed using the delta-delta
200 *CT* method (23). The comparative expression method generated data as
201 transcript fold change normalized to a constitutive reference gene transcript
202 (*ACT1*) and relative to the reference strain (*C. albicans* K1). The comparative
203 expression method generated data as transcript fold-change normalized to a
204 constitutive reference gene transcript (*ACT1*) and relative to planktonic *C.*

albicans, which were grown for 24 h in YPD at 37^{o}C with orbital shaking at 200 RPM.

RESULTS

Urinary catheter placement and animal well-being. Rats tolerated placement and infection of a urinary catheter well and did not show signs of illness throughout the course of the experiments, which extended for up to 72 hours. The animals continued normal intake of the food and water. No erythema or purulence was observed at the urethral exit site.

Time course analysis. To assess biofilm formation over time, the viable burden was determined using microbiological plate counts at various time points following *C. albicans* K1 infection of a rat urinary catheter. Pilot microbiological analysis showed involvement of numerous bacteria (data not shown). As the goal of the current project was to model a monomicrobial *C. albicans* biofilm, we elected to include antibiotic treatment to reduce the bacterial burden and produce a consistent fungal biofilm. Upon including the antibiotic regimen, we observed an increasing urinary *Candida* burden over the 24-72 h time period. The burden started at less than 10^3 CFU/ml at 24 h and ultimately reached 10^6 CFU/ml (**Figure 2A**). At the 48 h time point, the catheter viable burden was approximately 10^4 CFU/device (**Figure 2B**). On urinalysis, pyuria and hematuria were evident throughout the course of infection (**Table 1**). Hematuria occurred in rats with

uninfected catheters, suggesting this may be related to trauma. Pyuria was greater in rats with *C. albicans* infected catheters.

Scanning electron microscopy (SEM) of urinary catheter biofilms. We used SEM to assess biofilm extent and architecture of the in vivo *C. albicans* biofilms. SEM has been a valuable tool for examining biofilm cell morphology, extracellular matrix, and relative extent of biofilm formation (17, 24). After 48 h, a confluent layer of biofilm had covered most intraluminal surfaces. However, compared to the vascular catheter model, which employed a polyethylene catheter, the silicone urinary catheter biofilm was less resilient in the face of the processing required prior to SEM imaging (17). The biofilm was frequently observed peeling from the surface, a finding we suspect may have been related to the swelling of silicone during the dehydration process (**Figure 3**, 100x). At higher magnification, the mature biofilm was composed primarily of hyphae with an extracellular matrix material covering sections of the biofilm (**Figure 3**, 1500x). Due to the biofilm disruption observed with SEM processing, viable burden counts were utilized for comparisons of mutant strains and antifungal treatments in subsequent experiments.

Bladder microscopy. To discern the impact of the *C. albicans* urinary catheter infection on the host, we harvested the bladders for histology and SEM. H&E staining of the bladder revealed inflammation, marked by infiltration of polymorphonuclear cells (**Figure 4**). GMS staining for fungal elements confirmed

tissue invasion by *Candida*. Both yeast and hyphal forms were observed on the uroepithelial surface. The finding of fungal invasion and neutrophilic inflammation is consistent with acute cystitis. On SEM imaging of the bladder, the urothelial surface was covered by a heterogenous, fibrinous material (**Figure 5**). Given the density of this material, identification of the underlying cells was somewhat limited. Host blood cells could be identified. In several areas, there was the appearance of yeast beneath the extracellular material, suggesting the presence of a surface-associated biofilm infection (25).

Impact of antifungal drug treatments. Both in vitro and in vivo *Candida* biofilms exhibit tolerance to antifungal drugs (8, 17, 24, 26-32). We tested the impact of systemic administration of antifungal therapy on the in vivo urine catheter biofilm cell viability and bladder *Candida* viable burden. An azole (fluconazole) and amphotericin B were selected based on their achievable urinary concentrations and their clinical use for treatment of urinary candidiasis. An echinocandin was not included as minimal amounts of active drugs accumulate in the urine for this drug class. At the completion of the experiment, the urinary catheters of untreated animals contained nearly 5 $\log_{10}$ CFU/device (**Figure 6**). Treatment with either fluconazole (25 mg/kg/day) or amphotericin B deoxycholate (1 mg/kg/day) minimally impacted the catheter viable burden of *C. albicans*. However, these antifungal treatments decreased the viable fungal burden in the bladder, by approximately 2 and 3 $\log_{10}$ CFUs/bladder for

fluconazole and amphotericin B, respectively. The doses selected for study are typically effective in non-biofilm rodent infection models (19).

Transcriptional analysis of biofilm-associated cells. Approximately 0.3 µg of total RNA was isolated from a single urinary catheter, an amount sufficient to perform RNA analysis using many methods. To test the utility of the model for examination of *C. albicans* biofilm associated gene expression, we measured the transcript abundance of glucan-associated genes. These gene products have previously been shown to impact both biofilm matrix production and biofilm drug resistance in vitro and in a rat venous catheter model (21). Urinary catheter-associated biofilm cells were compared to free-floating, planktonic cells by RT-PCR (**Figure 7A**). Transcriptional analysis revealed that the glucan-associated genes were upregulated in urinary catheter-associated biofilm cells relative to planktonic cells, consistent with findings from the prior investigations of *C. albicans* biofilms. Of the transcripts measured, *BGL2* and *PHR1* were the most abundant, with 3-fold higher levels in the urinary catheter biofilm cells compared to planktonically grown *C. albicans*. Expression of *XOG1* and *FKS1* was greater in the biofilm condition, but less than 2-fold different.

Comparison of reference strain and adhesion defective mutant (*als1-/- als3-/-*). We next sought to test the ability of the model to detect the phenotype of a *Candida* strain with a biofilm deficient phenotype. We chose the *als1-/- als3-/-* mutant, which lacks two adhesins important for *C. albicans* adherence and

biofilm formation in vitro and in an in vivo vascular catheter model (33). We hypothesized that the mutant would also exhibit a biofilm defect in the rat urinary catheter niche. Compared to an otherwise isogenic reference strain, the *als1-/- als3-/-* urinary catheter biofilm was composed of nearly 100 fold fewer cells on viable burden testing (**Figure 7B**). As theorized based on prior biofilm studies, these adhesins appear to play a critical role in biofilm formation in the urine environment and this is detectable the rat urinary catheter model.

DISCUSSION

In the presence of an artificial substrate, *Candida* transitions to a biofilm lifestyle, engaging with the surface and proliferating as an adherent community (34-37). Numerous medical devices have been associated with biofilm growth and infection, including catheters (venous or urinary), vascular stents, cerebrospinal fluid shunts, pacemakers, and joint implants (36). Among these, CAUTIs represent 70% of all hospital acquired infections and *Candida* is the third most common CAUTI pathogen (38-40). Here, we characterize a rat urinary catheter biofilm infection model which is a close mimic of *Candida* CAUTI. The model recapitulates the clinical infection in terms of formation of a surface-associated biofilm, anatomic position of the catheter, conditions of the surrounding milieu, incorporation of host immune factors, material of the artificial device, and the flow conditions through the functioning catheter. With this model, we were able to quantify biofilm growth, assess biofilm architecture, study the impact of drug

317 therapy, analyze the biofilm transcriptome, compare the biofilm forming capacity
318 of mutant strains, and assess the host response to biofilm infection.
319
320 In vitro models of biofilm infection have been instrumental in many *Candida*
321 biofilm investigations, including the identification of factors governing biofilm
322 behaviors and their ability to tolerate antifungal therapy (28, 41-46). The models
323 can also be useful for characterizing the impact of surface modifications and
324 treatments. In vitro models have attempted to account for many in vivo infection
325 conditions suspected to be important in clinical infection. Examples include the
326 addition of urine to media to replicate the milieu of urinary biofilms, the
327 incorporation of substrate materials similar to medical devices, and the inclusion
328 of flow conditions (47). Uppuluri et al. examined *C. albicans* biofilm growth in the
329 presence of synthetic urine media that included defined electrolyte
330 concentrations, a relatively low pH, creatinine, and urea (47, 48). Similar to the
331 current investigation, biofilms formed under these conditions exhibited resistance
332 to antifungals commonly used to treat urinary tract infections, including
333 amphotericin B and fluconazole. However, compared to control biofilms growing
334 in RPMI media, biofilms produced under the synthetic urine media condition were
335 less dense and fewer cells had transitioned to the hyphal state. This is in contrast
336 to the current investigation, where hyphae were prominent in the *C. albicans*
337 biofilms on the luminal urinary catheter surface (**Figure 3**). Interestingly, the
338 antifungal therapy was effective against the tissue associated *Candida* in the
339 model suggesting the presence of both biofilm and non-biofilm cells in the model.

Differences between in vitro and in vivo models are not unexpected. It is difficult for in vitro models to account for all the factors which may be influencing biofilm infection in the host (49). For example, cells in the in vitro systems are not exposed to many immune components and proteins which may condition or coat the surface and promote adherence. Hundreds of proteins have been identified to adsorb to urinary devices in patients. The protein set is diverse and includes cytokeratins, albumin, and inflammatory proteins (50). These conditioning factors likely arise from surrounding cells under inflammatory conditions, as the protein content of urine is generally low. Mimicking this process in vitro would be very complex. In vitro conditions are also limited in the ability to reproduce the influence of the immune system, a dynamic process over the infection course.

While examining the utility of the model for gene expression analysis, we identified upregulation of several transcripts in the glucan synthesis and modification pathways in *C. albicans* urinary catheter biofilms (**Figure 7**). This was not surprising, given the role to these pathways in extracellular matrix production and biofilm drug resistance (21, 43). We found have similarities between our current study and our prior microarray analysis which compared rat vascular catheter biofilms to planktonic controls (51). For example, transcripts of β-1,3 glucan synthase, *FKS1*, were more abundant in the catheter biofilms (vascular 1.8-fold, urinary 1.3 fold). Likewise, 1,3-beta-glucosyltransferase, *BGL2,* was upregulated in both catheter models (vascular 1.5-3.1-fold, urinary 3.7-fold), as were glucanosyltransferase, *PHR1,* (vascular 2.4-24.2-fold, urinary

363 3.3-fold) and beta glucosidase, *XOG1,* (vascular 1.7-fold, urinary 1.9-fold). In a
364 rat denture model of *C. albicans* biofilm formation, *BGL2* was similarly
365 upregulated (1.6-fold) compared to planktonic controls (24). These findings
366 suggest there are conserved pathways among the various clinical biofilm niches.
367
368 Prior in vivo investigations of urinary catheter biofilms and CAUTI have utilized
369 rodent models. To examine *Pseudomonas aeruginosa* urinary catheter biofilms,
370 Kurosaka et al. developed a rat model of CAUTI. In this study, a stylet was
371 inserted through the urethra of a rat and a catheter segment was threaded over
372 the stylet and released into the bladder (52). Following transurethral inoculation,
373 bacterial biofilms were established on the catheter surfaces and animals
374 developed the histopathologic findings of acute pyelonephritis. This model was
375 subsequently adapted for use in a mouse for study of *Pseudomonas aeruginosa,*
376 *Proteus mirabilis, Enterococcus faecalis,* and *Candida albicans* (53-55). In an
377 investigation of *C. albicans* biofilms by Wang et al, the catheter segments were
378 secured in the bladder for 5-7 days prior to infection, allowing for host proteins to
379 adsorb of the device surface (55). In this model, dense biofilms formed on both
380 the luminal and external catheter surfaces and consisted of yeast and hyphae.
381 As a method to predispose to *Candida* infection, mice deficient in lysozyme M
382 production, an important effector for mucosal innate immunity, were utilized. The
383 advantages of the model include the smaller animal size of the mouse and the
384 ability to include the defined murine genotypes, such as the lysozyme M deficient
385 mouse.

One limitation of the previously described rodent CAUTI models is the placement of the catheter segments (53-55). Although the catheter segments are exposed to urine and host components in the bladder, the catheters lack a uretheral component and do not function to drain the urinary system, as would be the case for patient catheters. Without a urethral component, the catheters lack flow, one of the key factors influencing biofilm architecture and extracellular matrix production (56-58). To best account for physiologic flow in the current studies, we utilized urethral catheters that functioned to drain urine from the bladder throughout the course of the experiments. Not only did this have the advantage of mimicking flow, but also permitted repeated collection of urine samples.

To most closely mimic a patient infection, we chose to use a silicone urinary catheter, as this is the most common urinary catheter material (59). Biofilms formed on the luminal surface over the several days following intraluminal inoculation. However, on SEM, the biofilms were observed to often be dislodged or peeling from the catheter surface (**Figure 3**). This is in contrast to what has been observed in prior CAUTI model of *C. albicans* infection and a rat venous catheter biofilm infection, both of which had used polyethylene catheters (17, 55). We suspect the dehydration process required for SEM altered the silicone, weakening the biofilm binding. Another possibility is that urinary biofilms are less adherent to the device due to unique environmental conditions in the urine. We favor the former hypothesis given clinical descriptions of extensive biofilm in the literature and our demonstration of a large infectious burden by microbiological

counts. The viable plate count method was also useful for assessment of antifungal drug effect and the impact of various genetic mutants on urinary biofilm formation (**Figure 7**). Using this model we identified histopathologic changes consistent with acute cystitis (**Figure 4**). This is similar to descriptions from other animal models of bacterial CAUTI (52, 55). On specific fungal staining, mucosal invasion by *Candida* was evident and reminiscent of denture biofilm associated mucosal changes (**Figure 4**). The adherent community of *Candida* cells suggested the presence of a mucosal biofilm, as has been described for both oral and vaginal candidiasis (25, 60). On close examination of the bladder urothelial surface by SEM, we observed aggregates of cellular material encased in a fibrinous material, suggesting surface-associated biofilm formation (**Figure 5**). Similar findings have been described for *Klebsiella pneumonia* infection of a rat bladder (61). It has been proposed that epithelial cells are eventually sloughed during acute cystitis as a protective mechanism to rid the bladder of the surface-associated pathogens (61).

The current studies demonstrate the utility of the rat urinary catheter model for numerous research avenues involving *Candida* biofilm and CAUTI. Biofilm formation and architecture can be assessed by microscopy and assays can easily be designed to test the impact of antifungal drugs and the influence of gene products. The model allows for comparisons of genetically manipulated strains and transcriptional analysis. Given the physiologic catheter flow, it may be optimal for preclinical testing of catheters with impregnated or surface-adherent

anti-infectives (37). Although the focus of this study was *C. albicans*, the model could likely be adapted for use of non-albicans species, such as *C. parapsilosis*, *C. glabrata*, or *C. dubliniensis*, as has been described for other animal models (62, 63). Furthermore, comparisons among the various animal models of *Candida* biofilm infection may be of interest to identify pathways either unique to individual clinical niches or conserved among diverse clinical biofilms (17, 24, 25, 32, 55, 60, 64, 65).

ACKNOWLEDGEMENTS

We thank Aaron Mitchell and Clarissa Nobile for strain *als1-/- als3-/-*. This work was supported by the National Institutes of Health (R01 AI073289-01 and K08 AI108727) and the Burroughs Wellcome Fund. The authors acknowledge use of instrumentation supported by the UW MRSEC (DMR-1121288) and the UW NSEC (DMR-0832760).

REFERENCES

1. **Stamm WE.** 1991. Catheter-associated urinary tract infections: epidemiology, pathogenesis, and prevention. Am J Med. **91:**65S-71S.
2. **Tambyah PA, Knasinski V, Maki DG.** 2002. The direct costs of nosocomial catheter-associated urinary tract infection in the era of managed care. Infect Control Hosp Epidemiol. **23:**27-31.
3. **Richards MJ, Edwards JR, Culver DH, Gaynes RP.** 1999. Nosocomial infections in medical intensive care units in the United States. National Nosocomial Infections Surveillance System. Crit Care Med. **27:**887-892.
4. **Bouza E, San Juan R, Munoz P, Voss A, Kluytmans J, Co-operative Group of the European Study Group on Nosocomial I.** 2001. A European perspective on nosocomial urinary tract infections I. Report on the microbiology workload, etiology and antimicrobial susceptibility (ESGNI-003 study). European Study Group on Nosocomial Infections. Clin Microbiol Infect. **7:**523-531.

5. **Achkar JM, Fries BC.** 2010. *Candida* infections of the genitourinary tract. Clin Microbiol Rev. **23:**253-273.
6. **Kauffman CA.** 2014. Diagnosis and management of fungal urinary tract infection. Infect Dis Clin North Am. **28:**61-74.
7. **Saint S, Wiese J, Amory JK, Bernstein ML, Patel UD, Zemencuk JK, Bernstein SJ, Lipsky BA, Hofer TP.** 2000. Are physicians aware of which of their patients have indwelling urinary catheters? Am J Med. **109:**476-480.
8. **Chandra J, Kuhn DM, Mukherjee PK, Hoyer LL, McCormick T, Ghannoum MA.** 2001. Biofilm formation by the fungal pathogen *Candida albicans*: development, architecture, and drug resistance. J Bacteriol. **183:**5385-5394.
9. **Hawser SP, Douglas LJ.** 1994. Biofilm formation by *Candida* species on the surface of catheter materials in vitro. Infect Immun. **62:**915-921.
10. **Mah TF, Pitts B, Pellock B, Walker GC, Stewart PS, O'Toole GA.** 2003. A genetic basis for *Pseudomonas aeruginosa* biofilm antibiotic resistance. Nature. **426:**306-310.
11. **O'Toole GA.** 2003. To build a biofilm. J Bacteriol. **185:**2687-2689.
12. **Katragkou A, Simitsopoulou M, Chatzimoschou A, Georgiadou E, Walsh TJ, Roilides E.** 2011. Effects of interferon-gamma and granulocyte colony-stimulating factor on antifungal activity of human polymorphonuclear neutrophils against *Candida albicans* grown as biofilms or planktonic cells. Cytokine. **55:**330-334.
13. **Kauffman CA, Fisher JF, Sobel JD, Newman CA.** 2011. *Candida* urinary tract infections--diagnosis. Clin Infect Dis. **52 Suppl 6:**S452-456.
14. **Pappas PG, Kauffman CA, Andes D, Benjamin DK, Jr., Calandra TF, Edwards JE, Jr., Filler SG, Fisher JF, Kullberg BJ, Ostrosky-Zeichner L, Reboli AC, Rex JH, Walsh TJ, Sobel JD.** 2009. Clinical practice guidelines for the management of candidiasis: 2009 update by the Infectious Diseases Society of America. Clin Infect Dis. **48:**503-535.
15. **Maki DG, Tambyah PA.** 2001. Engineering out the risk for infection with urinary catheters. Emerg Infect Dis. **7:**342-347.
16. **Helbig S, Achkar JM, Jain N, Wang X, Gialanella P, Levi M, Fries BC.** 2013. Diagnosis and inflammatory response of patients with candiduria. Mycoses. **56:**61-69.
17. **Andes D, Nett J, Oschel P, Albrecht R, Marchillo K, Pitula A.** 2004. Development and characterization of an in vivo central venous catheter *Candida albicans* biofilm model. Infect Immun. **72:**6023-6031.
18. **Nobile CJ, Schneider HA, Nett JE, Sheppard DC, Filler SG, Andes DR, Mitchell AP.** 2008. Complementary adhesin function in *C. albicans* biofilm formation. Curr Biol. **18:**1017-1024.
19. **Andes D, van Ogtrop M.** 1999. Characterization and quantitation of the pharmacodynamics of fluconazole in a neutropenic murine disseminated candidiasis infection model. Antimicrob Agents Chemother. **43:**2116-2120.
20. **Jensen J, Warner T, Johnson C, Balish E.** 1996. Oral immunization of mice against candidiasis. J Infect Dis. **174:**133-140.

21. **Taff HT, Nett JE, Zarnowski R, Ross KM, Sanchez H, Cain MT, Hamaker J, Mitchell AP, Andes DR.** 2012. A *Candida* biofilm-induced pathway for matrix glucan delivery: implications for drug resistance. PLoS Pathog. **8:**e1002848.
22. **Nett JE, Sanchez H, Cain MT, Andes DR.** 2010. Genetic basis of *Candida* biofilm resistance due to drug-sequestering matrix glucan. J Infect Dis. **202:**171-175.
23. **Livak KJ, Schmittgen TD.** 2001. Analysis of relative gene expression data using real-time quantitative PCR and the 2(-Delta Delta C(T)) Method. Methods. **25:**402-408.
24. **Nett JE, Marchillo K, Spiegel CA, Andes DR.** 2010. Development and validation of an in vivo *Candida albicans* biofilm denture model. Infect Immun. **78:**3650-3659.
25. **Harriott MM, Lilly EA, Rodriguez TE, Fidel PL, Jr., Noverr MC.** 2010. *Candida albicans* forms biofilms on the vaginal mucosa. Microbiology. **156:**3635-3644.
26. **Khot PD, Suci PA, Miller RL, Nelson RD, Tyler BJ.** 2006. A small subpopulation of blastospores in *Candida albicans* biofilms exhibit resistance to amphotericin B associated with differential regulation of ergosterol and beta-1,6-glucan pathway genes. Antimicrob Agents Chemother. **50:**3708-3716.
27. **LaFleur MD, Kumamoto CA, Lewis K.** 2006. *Candida albicans* biofilms produce antifungal-tolerant persister cells. Antimicrob Agents Chemother. **50:**3839-3846.
28. **Mukherjee PK, Chandra J, Kuhn DM, Ghannoum MA.** 2003. Mechanism of fluconazole resistance in *Candida albicans* biofilms: phase-specific role of efflux pumps and membrane sterols. Infect Immun. **71:**4333-4340.
29. **Ramage G, Bachmann S, Patterson TF, Wickes BL, Lopez-Ribot JL.** 2002. Investigation of multidrug efflux pumps in relation to fluconazole resistance in *Candida albicans* biofilms. J Antimicrob Chemother. **49:**973-980.
30. **Kuhn DM, George T, Chandra J, Mukherjee PK, Ghannoum MA.** 2002. Antifungal susceptibility of *Candida* biofilms: unique efficacy of amphotericin B lipid formulations and echinocandins. Antimicrob Agents Chemother. **46:**1773-1780.
31. **Baillie GS, Douglas LJ.** 2000. Matrix polymers of *Candida biofilms* and their possible role in biofilm resistance to antifungal agents. J Antimicrob Chemother. **46:**397-403.
32. **Schinabeck MK, Long LA, Hossain MA, Chandra J, Mukherjee PK, Mohamed S, Ghannoum MA.** 2004. Rabbit model of *Candida albicans* biofilm infection: liposomal amphotericin B antifungal lock therapy. Antimicrob Agents Chemother. **48:**1727-1732.
33. **Nobile CJ, Andes DR, Nett JE, Smith FJ, Yue F, Phan QT, Edwards JE, Filler SG, Mitchell AP.** 2006. Critical role of Bcr1-dependent adhesins in *C. albicans* biofilm formation in vitro and in vivo. PLoS Pathog. **2:**e63.

34. **Donlan RM.** 2001. Biofilm formation: a clinically relevant microbiological process. Clin Infect Dis. **33:**1387-1392.
35. **Douglas LJ.** 2002. Medical importance of biofilms in *Candida infections*. Rev Iberoam Micol. **19:**139-143.
36. **Kojic EM, Darouiche RO.** 2004. *Candida* infections of medical devices. Clin Microbiol Rev. **17:**255-267.
37. **Tambyah PA, Halvorson KT, Maki DG.** 1999. A prospective study of pathogenesis of catheter-associated urinary tract infections. Mayo Clin Proc. **74:**131-136.
38. **Burton DC, Edwards JR, Srinivasan A, Fridkin SK, Gould CV.** 2011. Trends in catheter-associated urinary tract infections in adult intensive care units-United States, 1990-2007. Infect Control Hosp Epidemiol. **32:**748-756.
39. **Sievert DM, Ricks P, Edwards JR, Schneider A, Patel J, Srinivasan A, Kallen A, Limbago B, Fridkin S, National Healthcare Safety Network T, Participating NF.** 2013. Antimicrobial-resistant pathogens associated with healthcare-associated infections: summary of data reported to the National Healthcare Safety Network at the Centers for Disease Control and Prevention, 2009-2010. Infect Control Hosp Epidemiol. **34:**1-14.
40. **Dudeck MA, Horan TC, Peterson KD, Allen-Bridson K, Morrell G, Anttila A, Pollock DA, Edwards JR.** 2013. National Healthcare Safety Network report, data summary for 2011, device-associated module. Am J Infect Control. **41:**286-300.
41. **Chandra J, Mukherjee PK, Leidich SD, Faddoul FF, Hoyer LL, Douglas LJ, Ghannoum MA.** 2001. Antifungal resistance of candidal biofilms formed on denture acrylic in vitro. J Dent Res. **80:**903-908.
42. **Hawser SP, Douglas LJ.** 1995. Resistance of *Candida albicans* biofilms to antifungal agents in vitro. Antimicrob Agents Chemother. **39:**2128-2131.
43. **Nett J, Lincoln L, Marchillo K, Massey R, Holoyda K, Hoff B, VanHandel M, Andes D.** 2007. Putative role of beta-1,3 glucans in *Candida albicans* biofilm resistance. Antimicrob Agents Chemother. **51:**510-520.
44. **Kumamoto CA.** 2005. A contact-activated kinase signals *Candida albicans* invasive growth and biofilm development. Proc Natl Acad Sci U S A. **102:**5576-5581.
45. **Bachmann SP, Ramage G, VandeWalle K, Patterson TF, Wickes BL, Lopez-Ribot JL.** 2003. Antifungal combinations against *Candida albicans* biofilms in vitro. Antimicrob Agents Chemother. **47:**3657-3659.
46. **Nobile CJ, Mitchell AP.** 2005. Regulation of cell-surface genes and biofilm formation by the *C. albicans* transcription factor Bcr1p. Curr Biol. **15:**1150-1155.
47. **Uppuluri P, Dinakaran H, Thomas DP, Chaturvedi AK, Lopez-Ribot JL.** 2009. Characteristics of *Candida albicans* biofilms grown in a synthetic urine medium. J Clin Microbiol. **47:**4078-4083.

48. **Jain N, Kohli R, Cook E, Gialanella P, Chang T, Fries BC.** 2007. Biofilm formation by and antifungal susceptibility of *Candida* isolates from urine. Appl Environ Microbiol. **73:**1697-1703.
49. **Nett J, Andes D.** 2006. *Candida albicans* biofilm development, modeling a host-pathogen interaction. Curr Opin Microbiol. **9:**340-345.
50. **Elwood CN, Lo J, Chou E, Crowe A, Arsovska O, Adomat H, Miyaoka R, Tomlinson-Guns E, Monga M, Chew BH, Lange D.** 2013. Understanding urinary conditioning film components on ureteral stents: profiling protein components and evaluating their role in bacterial colonization. Biofouling. **29:**1115-1122.
51. **Nett JE, Lepak AJ, Marchillo K, Andes DR.** 2009. Time course global gene expression analysis of an in vivo *Candida* biofilm. J Infect Dis. **200:**307-313.
52. **Kurosaka Y, Ishida Y, Yamamura E, Takase H, Otani T, Kumon H.** 2001. A non-surgical rat model of foreign body-associated urinary tract infection with *Pseudomonas aeruginosa*. Microbiol Immunol. **45:**9-15.
53. **Kadurugamuwa JL, Modi K, Yu J, Francis KP, Purchio T, Contag PR.** 2005. Noninvasive biophotonic imaging for monitoring of catheter-associated urinary tract infections and therapy in mice. Infect Immun. **73:**3878-3887.
54. **Guiton PS, Hung CS, Hancock LE, Caparon MG, Hultgren SJ.** 2010. Enterococcal biofilm formation and virulence in an optimized murine model of foreign body-associated urinary tract infections. Infect Immun. **78:**4166-4175.
55. **Wang X, Fries BC.** 2011. A murine model for catheter-associated candiduria. J Med Microbiol. **60:**1523-1529.
56. **Uppuluri P, Chaturvedi AK, Lopez-Ribot JL.** 2009. Design of a simple model of *Candida albicans* biofilms formed under conditions of flow: development, architecture, and drug resistance. Mycopathologia. **168:**101-109.
57. **Al-Fattani MA, Douglas LJ.** 2004. Penetration of *Candida* biofilms by antifungal agents. Antimicrob Agents Chemother. **48:**3291-3297.
58. **Al-Fattani MA, Douglas LJ.** 2006. Biofilm matrix of *Candida albicans* and *Candida tropicalis*: chemical composition and role in drug resistance. J Med Microbiol. **55:**999-1008.
59. **Siddiq DM, Darouiche RO.** 2012. New strategies to prevent catheter-associated urinary tract infections. Nat Rev Urol. **9:**305-314.
60. **Dongari-Bagtzoglou A, Kashleva H, Dwivedi P, Diaz P, Vasilakos J.** 2009. Characterization of mucosal *Candida albicans* biofilms. PLoS One. **4:**e7967.
61. **Davis CP, Balish E, Mizutani K, Uehling DT.** 1977. Bladder response to *Klebsiella* infection: a scanning electron microscopy study. Invest Urol. **15:**227-231.
62. **Chen YL, Brand A, Morrison EL, Silao FG, Bigol UG, Malbas FF, Jr., Nett JE, Andes DR, Solis NV, Filler SG, Averette A, Heitman J.** 2011.

643 Calcineurin controls drug tolerance, hyphal growth, and virulence in
644 *Candida dubliniensis*. Eukaryot Cell. **10:**803-819.
645 63. **Nett J, Lincoln L, Marchillo K, Andes D.** 2007. Beta -1,3 glucan as a
646 test for central venous catheter biofilm infection. J Infect Dis. **195:**1705-
647 1712.
648 64. **Johnson CC, Yu A, Lee H, Fidel PL, Jr., Noverr MC.** 2012.
649 Development of a contemporary animal model of *Candida albicans*-
650 associated denture stomatitis using a novel intraoral denture system.
651 Infect Immun. **80:**1736-1743.
652 65. **Ricicova M, Kucharikova S, Tournu H, Hendrix J, Bujdakova H, Van**
653 **Eldere J, Lagrou K, Van Dijck P.** 2010. *Candida albicans* biofilm
654 formation in a new in vivo rat model. Microbiology. **156:**909-919.
655

656

657 **FIGURE LEGENDS**

658

659 **Figure 1**

660 **Model of a rat urinary catheter *C. albicans* biofilm infection.** A silicone
661 catheter (3.5 Fr) was inserted in the urethra of an anesthetized female rat (A). A
662 catheter covering and cone harness protect the urinary catheter (B).

663

664

665 **Figure 2**

666 ***C. albicans* burden in a rat urinary catheter biofilm.** Urine was collected from
667 a rat following *C. albicans* infection of an implanted urinary catheter after 24, 48,
668 and 72 hours of growth and microbiological counts were used to determine the
669 number of organisms present in the biofilms (A). Urinary catheters from 2 rats
670 were harvested after 48 h of biofilm growth and adherent *Candida* were
671 enumerated (B).

Figure 3

Scanning electron microscopy (SEM) images of a *C. albicans* urinary denture biofilm. Intact urinary catheter *C. albicans* biofilms were harvested after 48 h of growth, processed for SEM, and imaged. Scale bars for 100x and 1500x images represent 250 µm and 10 µm, respectively. Arrows point to areas of extracellular matrix. The arrow head denotes an area with hyphae and yeast.

Figure 4

Bladder histopathology for *C. albicans* urinary catheter biofilm infection. . Rat urinary catheters were infected with *C. albicans*. After 48 h, animals were sacrificed and dissected samples were fixed. Sections were stained with hematoxylin and eosin (H&E) and for *C. albicans* with Gomori's methenamine silver (GMS). Images were obtained at 10x and 40x. The outline box of the 10x images marks the approximate location where the 40x image was obtained.

Figure 5

Bladder SEM for *C. albicans* urinary catheter biofilm infection. Rat urinary catheters were infected with *C. albicans*. After 48 h, animals were sacrificed and dissected samples were processed for SEM and imaged. Scale bars represent 400 µm and 20 µm for 50x and 1000x images, respectively. Arrows point to yeast-like structures within the biofilm.

Figure 6

Impact of antifungal treatment on *C. albicans* urinary catheter biofilms. Rat urinary catheter biofilms were treated with either fluconazole (25 µg/ml subcutaneously once daily) or amphotericin B deoxycholate (1 mg/kg intraperitoneally) for 48 hours. Viable burden was determined by microbiological plate counts following disruption of the biofilm from the urinary catheter (A) or following bladder homogenization (B). Two rats were included for each condition in A and 1 rat was included for each condition for B. Microbiological replicates were performed in triplicate. ANOVA with pair-wise comparisons using the Holm-Sidak method was used to compare treatment viable burdens to untreated controls, *P<0.05. FLU=fluconazole, AMB=amphotericin B deoxycholate.

Figure 7

Role of select gene products in urinary *C. albicans* biofilm formation. (A) Transcriptional abundance of glucan associated genes in *C. albicans* urinary catheter biofilms. The transcript abundance of glucan modifying enzymes in urinary catheter biofilms was compared to planktonic *C. albicans*. Analysis of two rat catheters was performed in triplicate by RT-PCR with *ACT1* normalization. (B) Impact of adhesin disruption on urinary *C. albicans* biofilm formation. The biofilm forming capacity of *C. albicans als1-/- als3-/-* mutant and parent strain were compared with viable burden endpoint. One rat was used for each condition. Microbiological replicates were performed in triplicate. A Student's t test was used to compare viable burdens, *P<0.05.

718 **Table 1. Urinalysis in rats with *Candida albicans* urinary catheter-**
719 **associated biofilm infections.**

Duration of infection	*C. albicans* infected		uninfected (catheter only)	
	Leukocyte esterase	RBC	Leukocyte esterase	RBC
24 hours	15-70	+++	15	+++
48 hours	70+	+++	15	+++
72 hours	70+	+++	15	+++

720

721

722

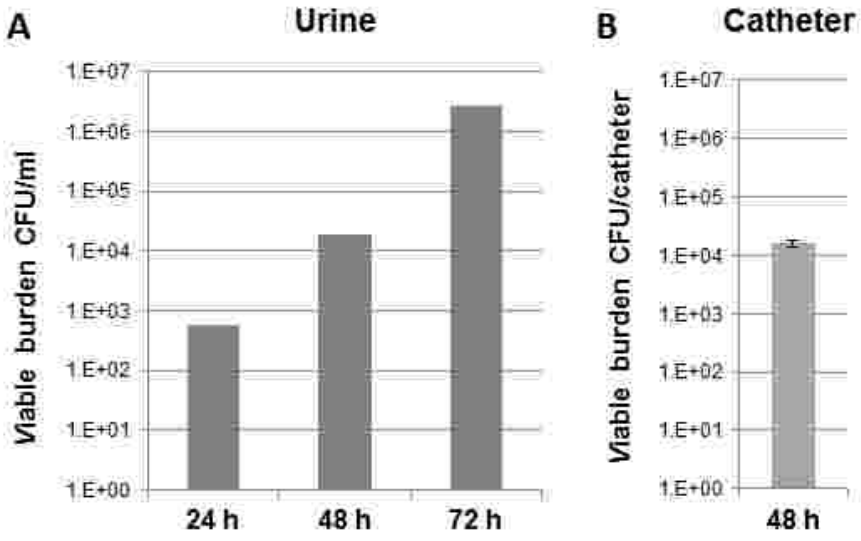

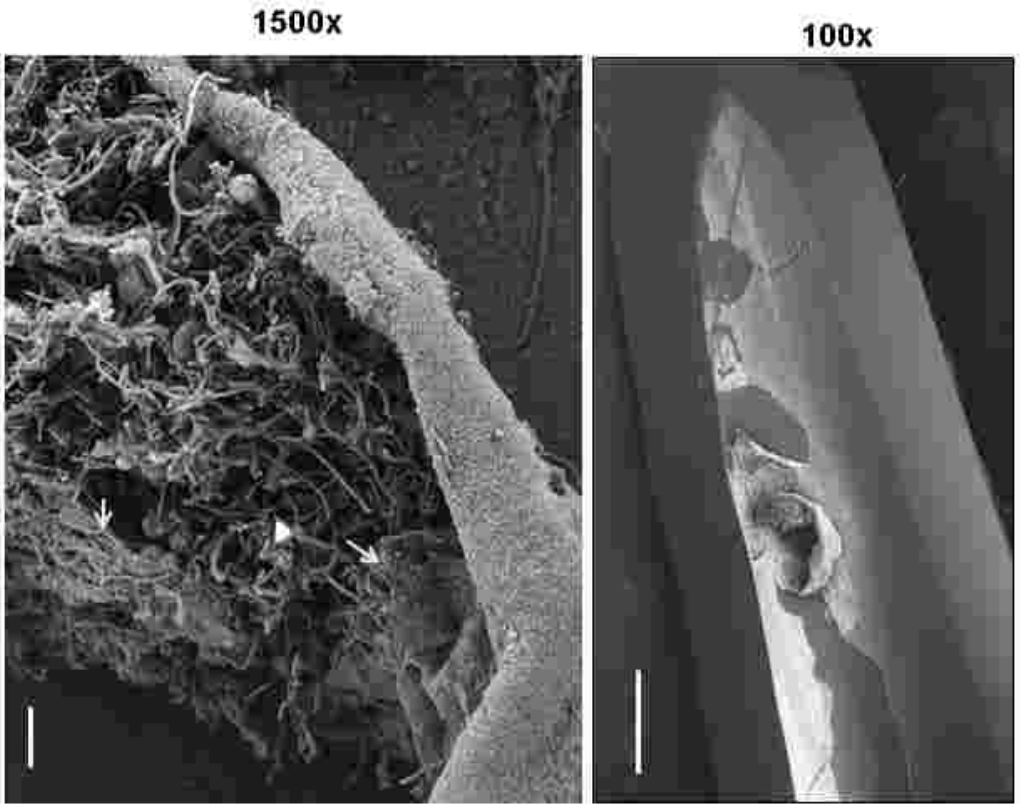
1500x
100x

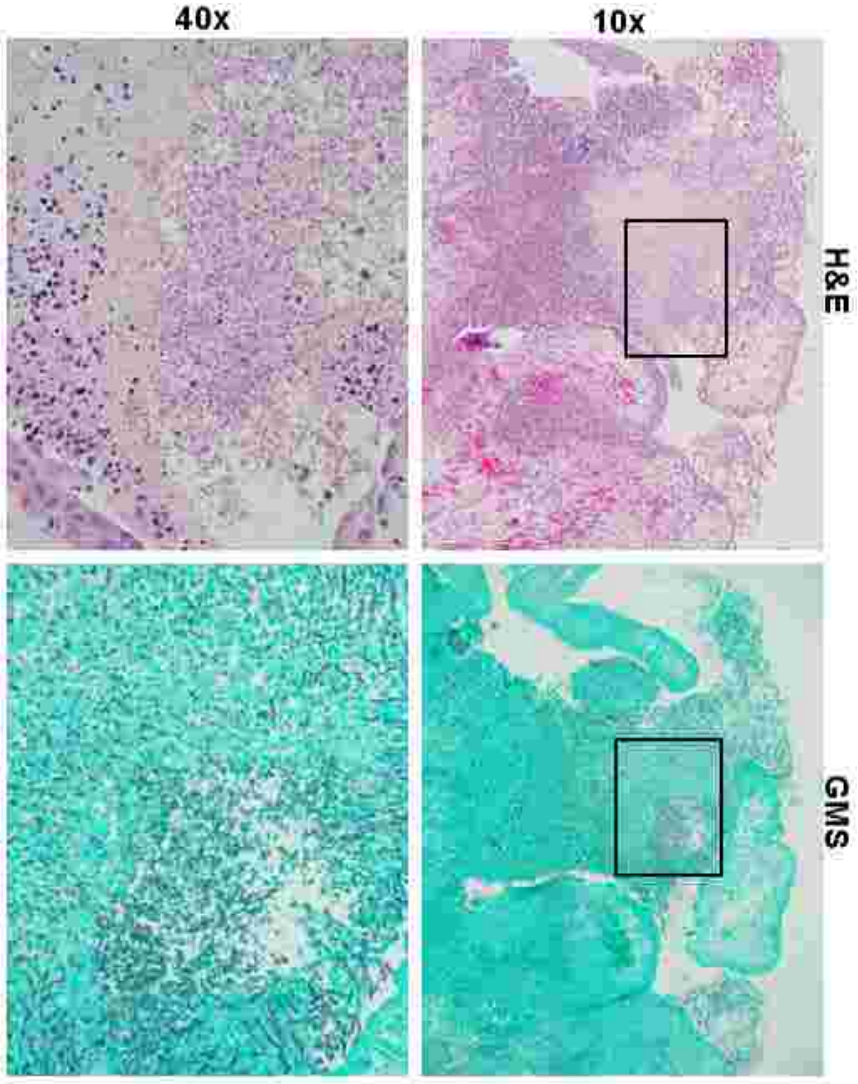
40x
10x
H&E
GMS

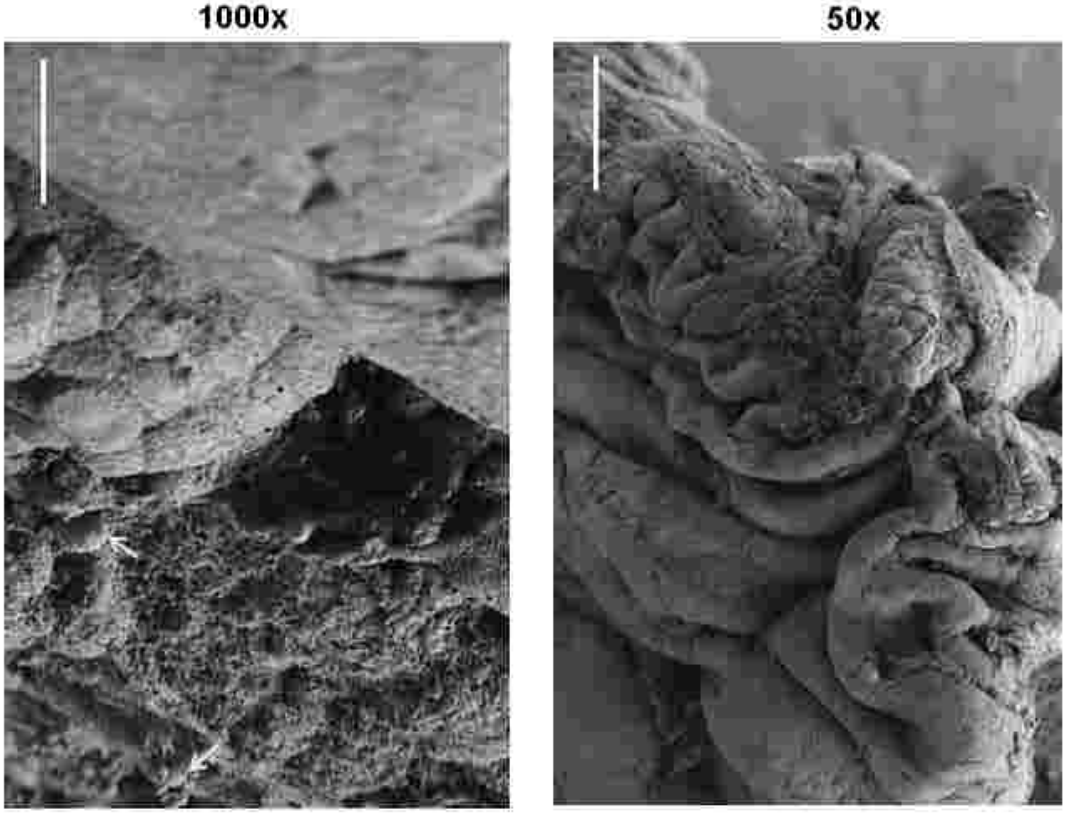
1000x
50x